

Microstructure and mechanical properties of powder metallurgy Ti-Al-Mo-V-Ag alloy

XIAO Dai-hong, YUAN Tie-chui, OU Xiao-qin, HE Yue-hui

State Key Laboratory of Powder Metallurgy, Central South University, Changsha 410083, China

Received 18 October 2010; accepted 18 November 2010

Abstract: The Ti-Al-Mo-V-Ag $\alpha+\beta$ alloys were processed by powder metallurgy (PM) using the blended elemental (BE) technique. The effects of Ag addition and sintering temperature on microstructure and properties of the Ti-5Al-4Mo-4V alloys were investigated using X-ray diffraction, optical microscope, scanning electron microscope and mechanical properties tests. The results show that adding Ag element increases the relative density and improves the mechanical properties of PM Ti-5Al-4Mo-4V alloy. After sintering at 1 250 °C for 4 h, the relative density and compression strength of Ti-5Al-4Mo-4V-5Ag alloy are 96.3% and 1 656 MPa, respectively.

Key words: titanium alloys; powder metallurgy (PM); Ag; microstructure; mechanical properties

1 Introduction

Titanium alloys have been widely used in military and civil fields, due to their low density, high specific strength, high yield-strength ratio, excellent plasticity and ductility, and good corrosion resistance [1–3]. However, the difficulty in extracting, melting and machining of titanium leads to high cost of production, and therefore restricts the wide applications of titanium alloys [4–5]. Powder metallurgy (PM) approaches are advantageous in producing near net shapes of components, and therefore largely increase the utilization ratio of materials and reduce machining cost [6]. Homogeneous and fine microstructure can be obtained by means of this way too. PM forming technology turns out to be a significant method for reducing costs of titanium alloys [4–5, 7]. The researches of titanium PM forming technology focus on the study of three methods: the blended elemental (BE), pre-alloying (PA), rapid solidification (RS), among which BE is much better than the other two methods either in economic benefit, component selection or the design of microstructure [8–9]. Products made from titanium alloys by BE are mainly applied in complex-shaped parts such as commercial titanium filters and impellers [7].

Aluminum has low density and high solid solubility in titanium (with a mass fraction more than 6%), which makes it one of the main alloying elements for titanium alloys [10–12]. The Ti-5Al-4Mo-4V (mass fraction, %) alloy prepared by cast processing and subsequent thermo-mechanical treatment is a high strength and heat resistant titanium alloy, and has been widely used in aerospace industry in Russia [1].

In this work, Ti-5Al-4Mo-4V powders with different Ag contents were consolidated to full density by vacuum sintering at high temperatures. The effects of addition of Ag on the microstructure and mechanical properties were investigated and compared with the samples without Ag additions.

2 Experimental

Table 1 shows the nominal composition of Ti-5Al-4Mo-4V alloys with different Ag contents. The raw materials include titanium powder (99.6%), molybdenum powder (99.5%), aluminum powder (99.5%), silver powder (99.7%), Al-V intermediate alloy powder (99.4%), with the average grain sizes of 48, 1.5, 2.6, 0.7 and 74 μm , respectively. Ag powders were added to Ti-5Al-4Mo-4V powders before milling. Mechanical milling was carried out for 48 h in 4 planetary ball

Foundation item: Project (PM2010) supported by State Key Laboratory of Powder Metallurgy Innovation Fund, China; Project (50825102) supported by the National Natural Science Foundation of China; Project (10JJ6066) supported by Natural Science Foundation of Hunan Province, China; Project (2009RS3025) supported by Hunan Science and Technology Plan, China

Corresponding author: XIAO Dai-hong; Tel: +86-731-88877880; E-mail: xdh0615@163.com
DOI: 10.1016/S1003-6326(11)60852-2

Table 1 Nominal composition of samples (mass fraction, %)

Sample	Al	Mo	V	Ag	Ti
Alloy 1	5	4	4	0	Bal.
Alloy 2	5	4	4	2	Bal.
Alloy 3	5	4	4	5	Bal.
Alloy 4	5	4	4	10	Bal.

milling system in alcohol under argon atmosphere. The ball to powder mass ratio was 5:1 and the milling speed was 350–400 r/min. After milling, the slurry was dried in a vacuum oven at 60 °C for 24 h. The mixed powders were granulated and pressed to compacts of 25 mm in diameter under a pressure of 200–300 MPa in a steel die. The compacts were put on a molybdenum piece and sintered at 1 150, 1 250 and 1 350 °C for 4 h in a vacuum sintering furnace, respectively. After sintering, the alloys were cooled to room temperature in the furnace.

The density of the sintered alloys was measured by Archimedes method. After being polished, the samples were corroded by Kroll reagent and observed using an optical microscope. Compression tests were carried out on a fully digital 3356 Instron testing machine at a speed of 1 mm/min. These samples were machined to size of $d5\text{ mm}\times 7\text{ mm}$. Fracture surface of the alloys after the compression tests was examined by FEI-Nano 230 field emission scanning electron microscopy (SEM) and the phase analysis was carried on a D/max2550pc X-ray diffractometer.

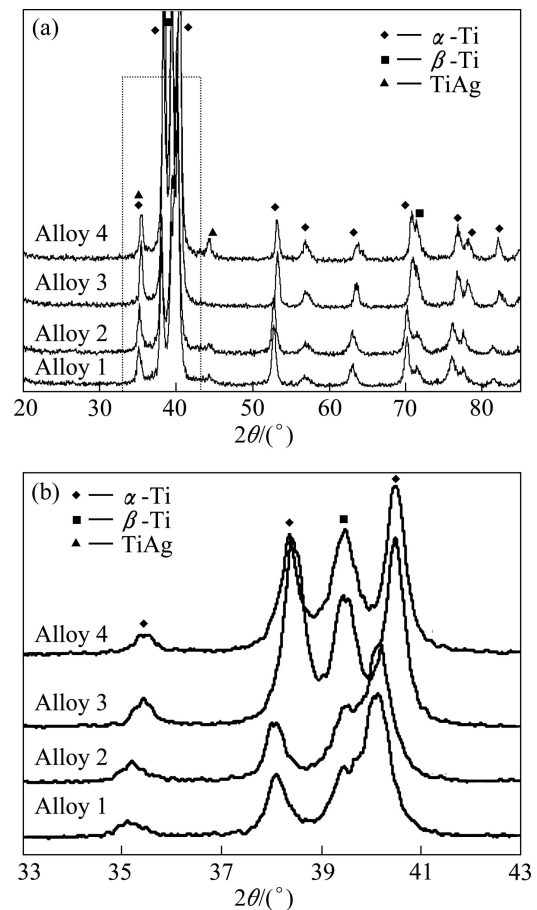
3 Results

3.1 Microstructures of sintered alloys

Figure 1 shows the XRD patterns of the alloys after sintering at 1 250 °C. It is found that the four alloys contain α and β phases. With increasing Ag content, the diffraction intensity of β phase increases. This indicates that Ag addition increases the volume fraction of β phase in the based alloys. Moreover, the 2θ angle of α phase shifts from low angle towards high angle direction, as can also be seen in the figure, indicating a change of the lattice parameter for alloys with the addition of Ag. Beside the diffraction peaks of α phase and β phase, there are also TiAg peaks in alloy 4.

Figures 2–4 show the microstructures of the samples sintered at different temperatures. The results show that the four alloys are all typical $\alpha+\beta$ microstructure and there are fine lamellar α phase and α colony. However, the microstructures vary apparently with different Ag additions.

Figure 2 shows the microstructure of the alloys after sintering at 1 150 °C. Increasing Ag content decreases the amount of pores in alloys, and increases the grain size slightly. There is not apparent difference between

**Fig. 1** XRD patterns of samples after sintering at 1 250 °C

the microstructures of alloys 1 and 2. They are typical $\alpha+\beta$ two phases, in which more equiaxed α phases occur (the white area in Fig. 2(a) and Fig. 2(b)). This indicates that 2% addition of Ag influences the microstructure of the based alloy. When adding 5% Ag, the microstructure of alloy 3 is mainly the Widmanstaetten structure, which consists of the primary β grains, lamellar α phases and colony α phases. The volume diffraction of the equiaxed α phase decreases (Fig.2(c)). With even more Ag added, alloy 4 is still mainly the Widmanstaetten structure consisting of primary β grains, lamellar α phase in β grains and α colony, and meanwhile there is minor amount of net-basketlike structure (Fig. 2(d)).

The microstructures of alloys 1 and 2 sintered at 1 250 °C (Fig. 3) are similar to the alloys sintered at 1 150 °C. The phases of the alloys 1 and 2 are $\alpha+\beta$ two phases, in which the equiaxed α phase is the main phase. Compared with the alloys sintered at 1 150 °C, alloy 3 has less the equiaxed α phase and more Widmanstaetten structure consisting of primary β grains, lamellar α phases and colony α phases. However, there is no any equiaxed α phase but the Widmanstaetten structure exists in alloy 4 (Fig. 3(d)). The thickness of lamellar α phases is smaller than that in alloy 3, and the amount of net-basketlike structure decreases too (Fig. 3(d)).

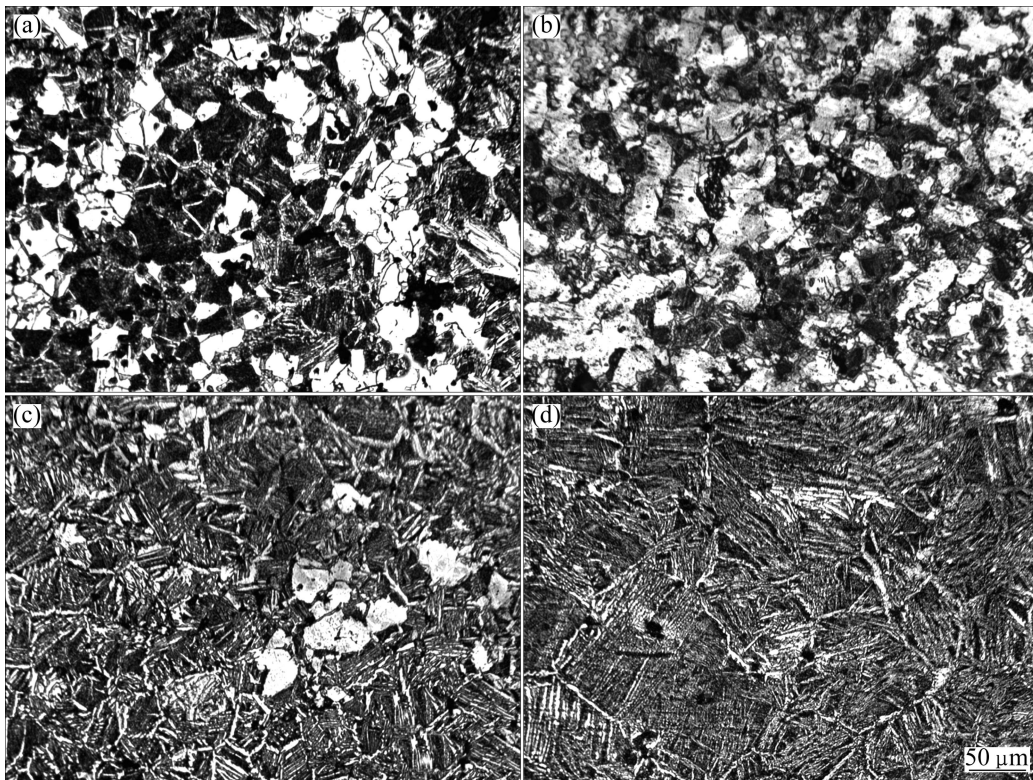


Fig. 2 Optical microstructures of samples after sintering at 1150 °C: (a) Alloy 1; (b) Alloy 2; (c) Alloy 3; (d) Alloy 4

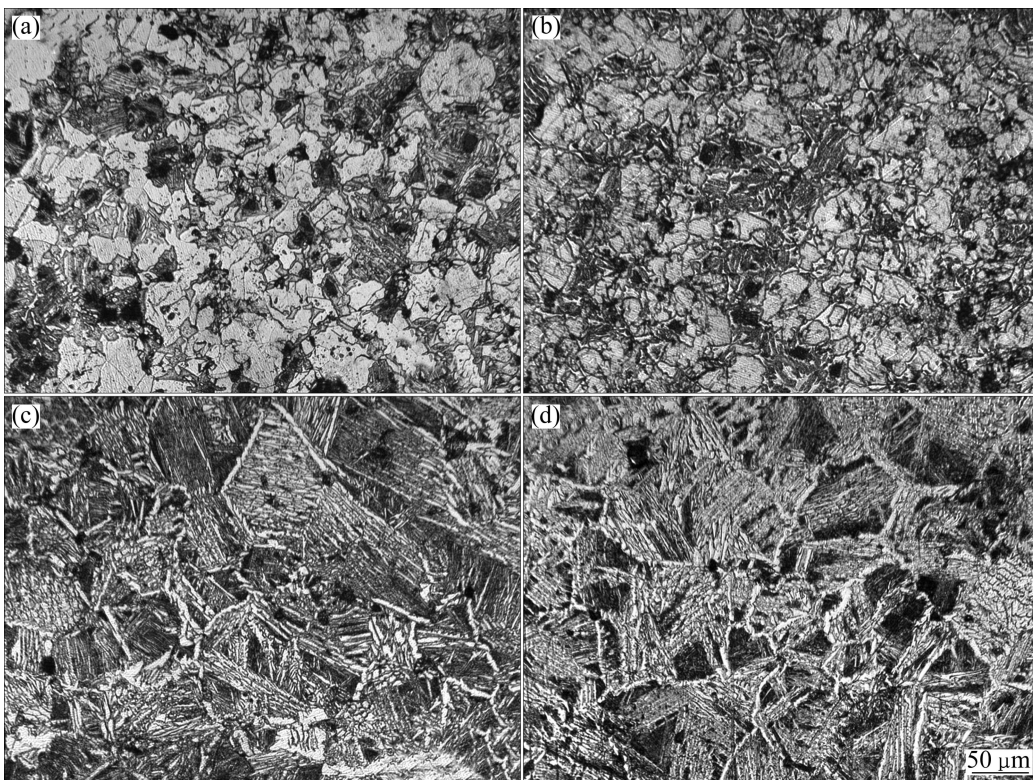


Fig. 3 Optical microstructures of samples after sintering at 1250 °C: (a) Alloy 1; (b) Alloy 2; (c) Alloy 3; (d) Alloy 4

Figure 4 shows the microstructures of the alloys sintered at 1350 °C. The microstructure of the alloys 1 and 2 is a $\alpha+\beta$ two phases, in which the equiaxed α phase

is the dominating phase. At the same time, the grain size increases as well as the lamellar α phase. However, alloy 3 apparently has the Widmanstaetten structure consisting

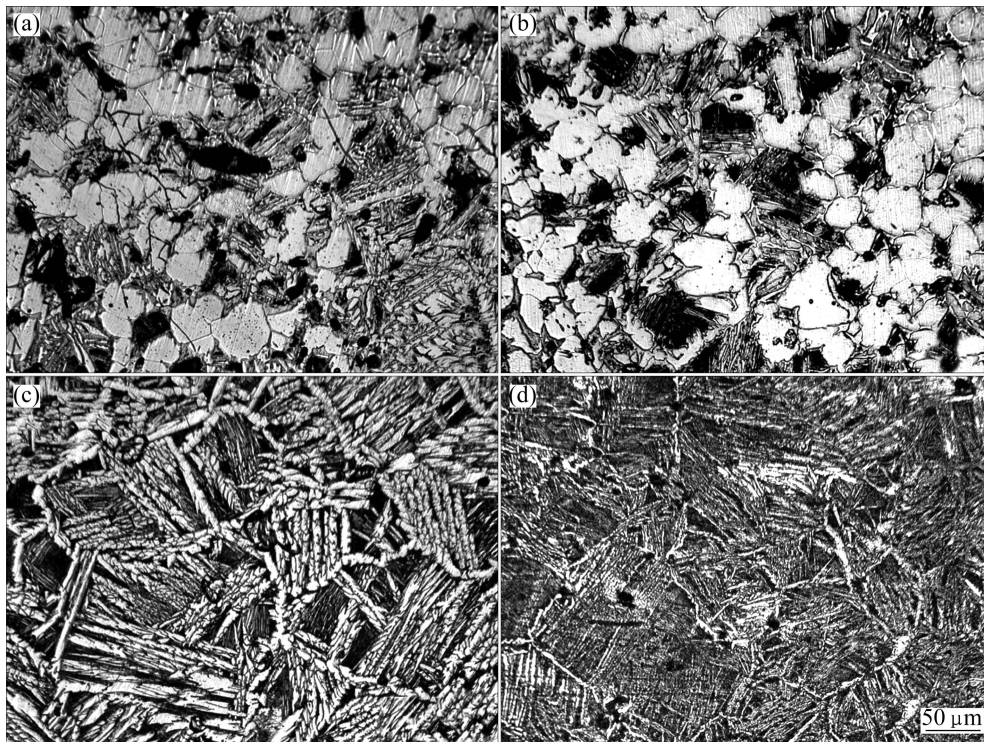


Fig. 4 Optical microstructures of samples after sintering at 1350 °C: (a) Alloy 1; (b) Alloy 2; (c) Alloy 3; (d) Alloy 4

of primary β grains, lamellar α phases and colony α phases, among which the thickness of lamellar α phase is comparatively bigger. Alloy 4 has the similar microstructure to alloys sintered at 1250 °C, but decreased thickness of α phase at boundaries of primary β grains as well as decreased α colony size.

3.2 Mechanical properties

Figure 5 shows the properties of the sintered alloys. With increasing Ag content, the relative density of alloys sintered at 1150 °C increases from 82.5% (alloy 1) to 93.6% (alloy 4). The compression property testing shows that the compressive strength of alloy 1 without Ag is 1002 MPa, with a compression rate of 2.1%. The compressive strength and compression rate of alloy 2 with 2% Ag is 1244 MPa and 6.2%, respectively. With further increasing Ag content to 5%, the compressive strength of alloy 3, compared with that of alloy 1, is increased by 578 MPa, and the compression rate reaches 25%. The compressive strength and compression rate of the alloy with 10% Ag reach 1476 MPa and 21%, respectively.

The relative densities of the four alloys sintered at 1250 °C, which are 85%, 88%, 95% and 96%, respectively, increase compared with those of the alloys sintered at 1150 °C. The compression property testing indicates that the compressive strength of matrix alloys increases apparently with increasing Ag content, from 1134 MPa to 1568 MPa. And the compression rate

increases from 1.5% to 19.2%. Besides, the comparison between 1150 °C and 1250 °C shows that increasing sintering temperature improves the compressive strength while decreases the compressive rate.

With increasing Ag content, the relative density of the alloys increases to 93.6% (alloy 2), 95.3% (alloy 3) and 97.1% (alloy 4), respectively. The compression property testing shows that the compressive strength of alloy 1 (1231 MPa) sintered at 1350 °C is slightly improved compared with that of the alloys sintered at 1250 °C. The compressive strength of the other three alloys with Ag content is higher than that of alloy 1, and the strength of alloy 4 exceeds that of alloy 3. However, compared with the samples sintered at 1250 °C, the compressive strength and compression rate of the alloys with the same alloying constituents decrease, which indicates that increasing sintering temperature is disadvantageous for the compression property of powder metallurgy titanium alloys.

Figure 6 shows the typical compression stress—strain curves of the four alloys sintered at different temperatures. By adding 5%–10% Ag, the sintered alloys shows apparent plastic deformation stage, indicating that the alloys are highly resistant to plastic deformation. The high plastic deformation ability can avoid sudden fracture of alloys in actual working condition. In addition, after sintering at different temperatures, the alloys have high compress modulus.

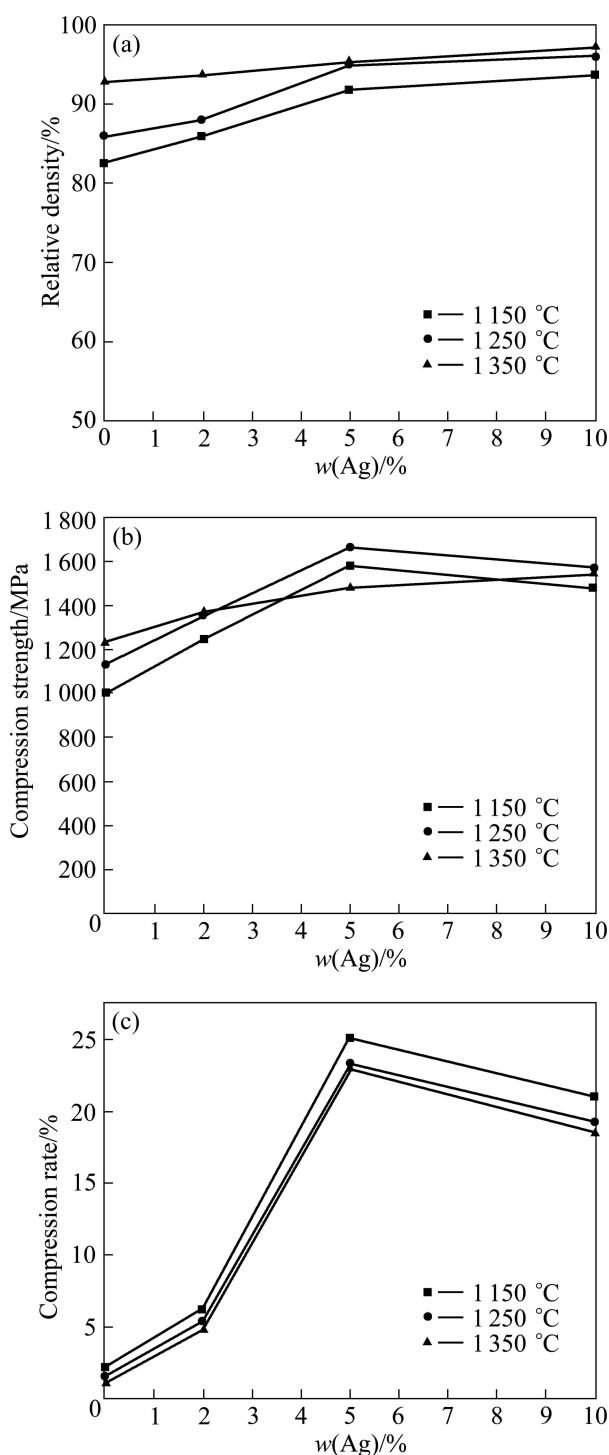


Fig. 5 Properties of samples after sintering at different temperatures: (a) Relative density; (b) Compression strength; (c) Compressive rate

3.3 Fracture analysis

Figure 7 shows the microstructures of the compression fracture surface of alloys 1 and 4 sintered at 1 250 °C and 1 350 °C, respectively. The amount of pores on the fracture surface decreases apparently with the increase of Ag content, which confirms the results in Figs. 4 and 5. The fracture modes are mainly

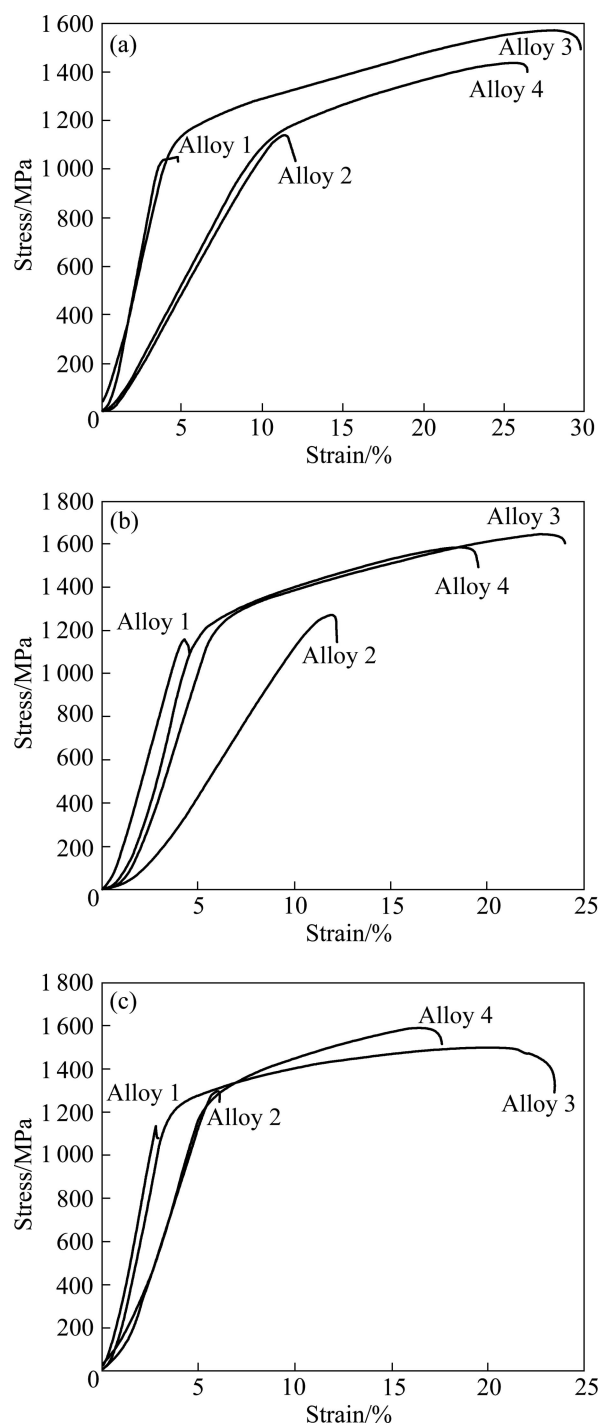


Fig. 6 Compressive stress—strain curves of samples after sintering at different temperatures: (a) 1 150 °C; (b) 1 250 °C; (c) 1 350 °C

transgranular fracture. Meanwhile, there is obvious lamellar structure and the lamellar structure has the colony α phases in the alloy 3. SEM observation on α colony (Fig. 8) shows that the colony α phases consist of lamellar structure with an average size of 120 nm, and between the lamellas there are nanometer spherical TiAg compounds, which can contribute to the dispersion strengthening of the alloy 3.

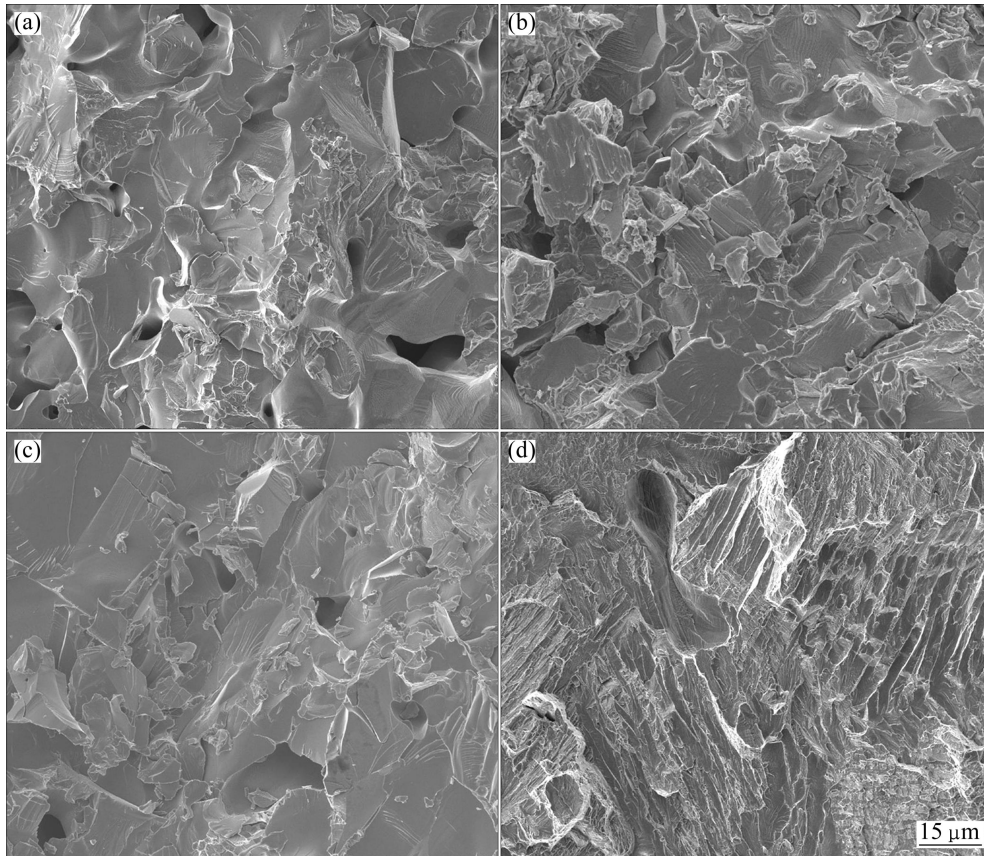


Fig. 7 SEM images of fracture surface of alloys 1(a, b) and 4 (c, d) after sintering at 1 250 °C (a, c) and 1 350 °C (b, d)

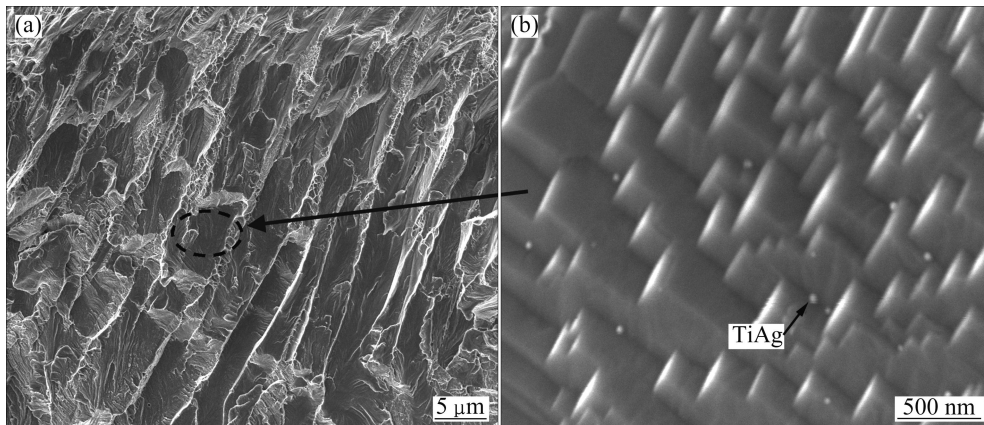


Fig. 8 SEM images of fracture surface of alloy 4 after sintering at 1 350 °C

4 Discussion

The properties of powder metallurgy titanium alloys can be affected by alloying constituents, porosity and microstructure. Ti-5Al-4Mo-4V alloys are typical $\alpha+\beta$ microstructures. Aluminum is the α -stability element, while Mo and V act as the β -stability elements. All these elements are dissolved in α and β phases and can contribute to the effect of solid solution strengthening. Moreover, they also change the phase proportion in the

powder metallurgy titanium alloys. Ag is an eutectoid β -stability element, which can strengthen the solid solution. However, when the content of Ag exceeds certain amount, eutectoid transformation takes place between the excessive Ag and Ti, and produces TiAg compounds (Fig. 1). This violently decreases the transformation temperature of $(\alpha + \beta)/\beta$ phases and makes it easy for the generation of lamellar structure in alloys [12–15]. The results of Figs. 2–5 indicate that the dominating structure in the alloys consists of primary β grains, lamellate α phase in β grains and α colony.

In the Ti-5Al-4Mo-4V-(5–10)Ag alloy system, the alloys located in two-phase region were cooled to room temperature in furnace from β phase region. During the cooling stage, crystal nucleus was formed at the boundaries and grew into crystal boundaries, due to the small supercooling degree. Then, a large amount of nucleus in the region of grain boundaries grew towards the inner grains and formed parallel lamellar α phase with the same orientation. On the other hand, nucleus can also be formed inside the grains and grew into α colony. The size and quantity of α colony are affected by many factors. Higher heating temperature, longer holding time, more β -stability elements, lower β phase transformation point and less cooling rate make larger α colony. The quantity of α colony in alloy 4 surpasses that of alloys 3 and 2 apparently, mainly due to the high Ag content of β -stability elements. Figures 2–4 also show that the amount of the equiaxed α phases in alloy 3 decreases while the Widmanstaetten structure decreases. This is attributed to the increasing diffusion rate of the β -stability elements (Mo, V, Ag) with the improvement of sintering temperature. And therefore solution is more adequate in the subsequent furnace cooling process, and α phases precipitate from primary β phase to form fine lamellar Widmanstaetten structure.

In addition, Figure 5 shows that the relative density of the sintered alloys increases with the sintering temperature and can reach as high as 97%, due to the high powder activity at high sintering temperature. And the greater diffusion rate of β -stability elements (Mo, V, Ag), faster shrinkage of the sintered alloys and less porosity promote the relative density of the sintered alloys. At the same time, the addition of Ag can lower the $(\alpha + \beta)/\beta$ phase transformation point, thus lower the sintering temperature of composite powder. Nano-scale TiAg compounds generated during sintering can also prevent the grain growth so as to raise the relative density of the sintered alloys containing Ag.

Figures 5 and 6 show that, the properties of the sintered alloys with different Ag contents are different. With the increase of Ag content, porosity decreases with the increase of relative densities of alloys (Figure 5) under the same sintering process. And compressing strength and plastic deformation capacity increase with the increase of Ag content. Especially with 5%–10% Ag content, the compressing strength of the alloys is over 1 400 MPa and the compression rate also becomes more than 19% under 1 250–1 350 °C sintering temperature. The relationship between strength and density of the alloys can be expressed using the following formula [16]:

$$\sigma_m = \sigma_0 \exp(-bm) \quad (1)$$

where σ_m is the corrected tensile strength, σ_0 is the real

tensile strength of the alloy having certain porosity m , and b is a constant of about 4–7. We can see that, with the decrease of porosity m , σ_m of the sintered titanium alloy performs exponential growth trend. From Figs. 1 and 5, adding high content Ag improves the relatively density of the sintered alloys, and changes the phase composition of the based alloy. The microstructures of alloys change from $\alpha + \beta$ phase microstructure to the Widmanstaetten structure, while nano-scale TiAg compound also is generated, and the compression strength is improved.

5 Conclusions

1) Ti-5Al-4Mo-4V alloys with 5%–10% Ag were prepared by BE technique. The addition of Ag can improve the relative density and the compression properties.

2) By increasing the sintering temperature, the relative density of the sintered titanium alloys can reach 96%, the compressive strength is over 1 500 MPa and the compression rate can reach more than 19%.

3) When adding 5%–10% Ag into the based alloy, the microstructure of sintered alloys changes from typical $\alpha + \beta$ two phases to the Widmanstaetten structure. Meanwhile, nano-scale TiAg compound is generated in the matrix alloys, acting as dispersion strengthening.

References

- [1] LEYENS C, PETERS M. Titanium and titanium alloys [M]. Weinheim: Wiley-VCH Verlag GmbH & Co. KGaA, 2003: 351–368.
- [2] JACKSON M. Titanium—21st century metal in transition [J]. Materials World, 2007, 15(5): 32–34.
- [3] VALENTIN N M. Titanium alloys Russian aircraft and aerospace applications [M]. Taylor & Francis Group, LLC, 2008: 147–153.
- [4] TANG Hui-min, LIU Yong, WEI Wei-feng, CHEN Li-fang. Effect of rare-earth element addition on microstructure and mechanical properties of P/M titanium alloys [J]. The Chinese Journal of Nonferrous Metals, 2004, 14(2): 244–249. (in Chinese)
- [5] HANSON A D, RUNKLE J C, WIDMER R, HEBEISEN J C. Titanium near net shapes from elemental powder blends [J]. International Journal of Powder Metallurgy, 1990, 26(2): 157–164.
- [6] KIPOUROS G J, CALEY W F, BISHOP P. On the advantages of using powder metallurgy in new light metal alloy design [J]. Metallurgical and Materials Transactions A, 2006, 37(12): 3429–3436.
- [7] FROES F H, EYLON D. Powder metallurgy of titanium alloys [J]. International Materials Reviews, 1990, 35(3): 162–182.
- [8] ROBERTSON I M, SCHAFFER G B. Design of titanium alloy for efficient sintering to low porosity [J]. Powder Metallurgy, 2009, 52(4): 311–315.
- [9] TAKAHIRO F, OGAWA A, OUCHI C, TAJIMA H. Microstructure and properties of titanium alloy produced in the newly developed blended elemental powder metallurgy process [J]. Materials Science and Engineering A, 1996, 213(1–2): 148–153.
- [10] TAMIRISAKANDALA S, BHAT R B, RAVI V A. Powder metallurgy Ti-6Al-4V-xB alloys: Processing, microstructure, and properties [J]. JOM, 2004, 56(5): 60–63.

- [11] AZEVEDO C R F, RODRIGUES D, NETO F B. Ti-Al-V powder metallurgy (PM) via the hydrogenation dehydrogenation (HDH) process [J]. Journal of Alloys and Compounds, 2003, 353(1–2): 217–227.
- [12] IVASISHIN O M, SAVVAKIN D G, FROES F, MOKSON V C. Synthesis of alloy Ti-6Al-4V with low residual porosity by a powder metallurgy method [J]. Powder Metallurgy and Metal Ceramics, 2002, 41(7–8): 382–90.
- [13] GRINDNEV V N, IVASHISHIN O M, MARKOVSKII P E. Influence of heating rate on the temperature of the $(\alpha+\beta)\rightarrow\beta$ -transformation of titanium alloys [J]. Metal Science and Heat Treatment, 1985, 27(1–2): 43–48.
- [14] KIM J Y, SHIM I O, HONG S Y. Effect of initial lamellar structure on globularization of hot multi-forged ELI grade Ti-6Al-4V alloy [J]. Materials Science Forum, 2007, 558–559(1): 529–532.
- [15] MO Wei. Titanium [M]. Beijing: Metallurgical Industry Press, 2008, 252–257. (in Chinese)
- [16] DUCKWORTH W. Discussion of ryshkewitch paper [J]. J Amer Ceramic Soc, 1953, 36: 68–75.

粉末冶金 Ti-Al-Mo-V-Ag 合金的显微组织与力学性能

肖代红, 袁铁锤, 欧小琴, 贺跃辉

中南大学 粉末冶金国家重点实验室, 长沙 410083

摘要: 通过粉末冶金元素混合法, 制备含 α 及 β 相的 Ti-Al-Mo-V-Ag 合金。通过 X 射线衍射、金相观察、扫描电镜观察及力学性能测试, 研究 Ag 的添加及烧结温度对 Ti-5Al-4Mo-4V 合金的组织与性能影响。结果表明: Ag 的添加能提高粉末冶金 Ti-5Al-4Mo-4V 合金的相对密度, 改善合金的力学性能; 在 1 250 °C 下烧结 4 h 后, Ti-5Al-4Mo-4V-5Ag 合金的相对密度及抗压强度分别达到 96.3% 和 1 656 MPa。

关键词: 钛合金; 粉末冶金; 银; 显微组织; 力学性能

(Edited by LI Xiang-qun)